



**HAL**  
open science

## **Anomalous conductivity in PZT thin film deposited on copper substrate electrode**

Andrei Th Ionescu, Anca-Luiza Alexe-Ionescu, Salvatore Marino, Marco Castriota, Giuseppe Strangi, Gaetano Nicastro, Nicola Scaramuzza

► **To cite this version:**

Andrei Th Ionescu, Anca-Luiza Alexe-Ionescu, Salvatore Marino, Marco Castriota, Giuseppe Strangi, et al.. Anomalous conductivity in PZT thin film deposited on copper substrate electrode. *Philosophical Magazine*, 2010, 90 (13), pp.1733-1742. 10.1080/14786430903463529 . hal-00587294

**HAL Id: hal-00587294**

**<https://hal.science/hal-00587294>**

Submitted on 20 Apr 2011

**HAL** is a multi-disciplinary open access archive for the deposit and dissemination of scientific research documents, whether they are published or not. The documents may come from teaching and research institutions in France or abroad, or from public or private research centers.

L'archive ouverte pluridisciplinaire **HAL**, est destinée au dépôt et à la diffusion de documents scientifiques de niveau recherche, publiés ou non, émanant des établissements d'enseignement et de recherche français ou étrangers, des laboratoires publics ou privés.



**Anomalous conductivity in PZT thin film deposited on copper substrate electrode**

Journal:	<i>Philosophical Magazine &amp; Philosophical Magazine Letters</i>
Manuscript ID:	TPHM-09-Jul-0293.R1
Journal Selection:	Philosophical Magazine
Date Submitted by the Author:	16-Oct-2009
Complete List of Authors:	Ionescu, Andrei; Universitatea din Bucuresti, Facultatea de Fizica Alexe-Ionescu, Anca-Luiza; Universitatea "Politehnica" din Bucuresti, Departamentul de Fizica marino, salvatore; University of Calabria, department of physics castriota, marco; University of Calabria, department of physics strangi, giuseppe; University of Calabria, department of physics nicastro, gaetano; University of Calabria, department of physics Scaramuzza, Nicola; University of Calabria, department of physics
Keywords:	ferroelectrics, copper, electrical conductivity, films, interfaces
Keywords (user supplied):	



1 **Anomalous conductivity in PZT thin film deposited on copper**  
2  
3  
4 **substrate electrode.**  
5  
6  
7  
8  
9

10  
11 Andrei Th. Ionescu<sup>a</sup>, Anca-Luiza Alexe-Ionescu<sup>b</sup>, Salvatore Marino<sup>c</sup>, Marco  
12  
13 Castriota<sup>c</sup>, Giuseppe Strangi<sup>c</sup>, Gaetano Nicastro<sup>c</sup> and Nicola Scaramuzza<sup>c,\*</sup>  
14  
15  
16  
17  
18  
19  
20

21 a) Facultatea de Fizica, Universitatea din Bucuresti, P.O.B MG-11, Ro-077125  
22  
23 Bucharest, Romania  
24  
25

26 b) Departamentul de Fizica, Universitatea “Politehnica” din Bucuresti, Splaiul  
27  
28 Independentei 313, Ro-060042 Bucharest, Romania  
29  
30

31 c) INFM-CNR-LICRYL Laboratory-CEMIF.CAL, Department of Physics University  
32  
33 of Calabria, Via P. Bucci, Cubo 33B, 87036 Rende (CS) Italy  
34  
35  
36

37 \*) Corresponding author. Tel.: (+39) 0984-496113 Fax. (+39) 0984-494401 E-mail:  
38  
39 scaramuzza@fis.unical.it  
40  
41  
42  
43  
44  
45  
46  
47  
48  
49  
50  
51  
52  
53  
54  
55  
56  
57  
58  
59  
60

## Abstract

Electrical properties of ferroelectric films are influenced by many factors among which the methods of synthesizing the ferroelectric film itself and the characteristics of the substrate electrode. Conductivity measurements were performed on PZT (lead zirconate titanate) thin films deposited by sol-gel synthesis on a copper electrode aiming to investigate the electric properties and to individuate the predominant charge carriers of such samples. A semiconducting PZT/Cu interface appears during the thermal treatment influencing severely the electric conduction. A power law, describing the transport mechanism across PZT film, has been found empirically.

## 1. Introduction

Thin films of lead zirconate titanate are of great scientific and technological interest, especially during the last decade, because of their application in non volatile memories, sensors and, more recently, in asymmetric nematic liquid crystal cells [1-3]. Moreover, the problems associated with the applications of ferroelectrics such as: polarization fatigue, field and frequency dependence of the piezoelectrics, elastic and dielectric properties, have produced an intensive research on the fundamental properties of ferroelectric materials.

One of the main aspects in understanding the behaviour of ferroelectric films is the interaction with the substrate material used as electrode. Platinum is the most popular substrate for ferroelectric materials because of its good resistance to oxidation. Otherwise, conducting oxide electrodes such as  $\text{RuO}_2$  [4],  $\text{IrO}_2$ [5] or ITO[6] have been widely used.

In the present work a  $[\text{Pb}(\text{Zr}_{0.53}\text{Ti}_{0.47})\text{O}_3]$  (PZT) thin film obtained by sol-gel procedure has been deposited on a copper electrode by spin coating and, subsequently, submitted to annealing at  $600^\circ\text{C}$  for 1h to ensure the transition to the ferroelectric perovskite phase. Interesting hypotheses about the sign and the mobility of the charge carriers have been drawn from the electrical measurements done upon this sample.

## 2. Experimental Details

Lead Zirconate Titanate (PZT) thin films were obtained by hybrid (carboxylate and alkoxides) sol-gel route and by spin coating deposition of the obtained mother

1 solution on a copper substrate. The reagents used, supplied by Sigma-Aldrich, are:  
2  
3  
4 Lead(II) acetate trihydrate ( 99.999 %), Zirconium(IV) propoxide solution (70 wt. %  
5  
6 in 1-propanol), Titanium(IV) isopropoxide ( 99.999 %), Acetic acid glacial (99.99+  
7  
8 %), n-Propanol anhydrous (99.7%), Ethylene glycol anhydrous (99.8%).  
9  
10

11 The synthesis of the mother solution has been performed in “humidity free” Glove  
12  
13 Box in Argon atmosphere (concentration of humidity and of molecular oxygen lower  
14  
15 than 1 ppm). Briefly, in order to obtain stable mother solution, 10.43 g of  
16  
17 Pb(CH<sub>3</sub>COO)<sub>2</sub>·3H<sub>2</sub>O have been dissolved in CH<sub>3</sub>COOH. The amount of acetic acid  
18  
19 was chosen to have its mole number twice the sum of the mole number of lead,  
20  
21 zirconium, and titanium. When the Lead(II) acetate trihydrate is completely  
22  
23 dissolved, stoichiometric amounts of Zr(C<sub>3</sub>H<sub>7</sub>O)<sub>4</sub> and Ti[(CH<sub>3</sub>)<sub>2</sub>CHO]<sub>4</sub> solutions  
24  
25 have been added, taking care to the temperature of the solution. Finally, when the  
26  
27 solution is cooled down at room temperature, acetic acid, n-propanol (23.10 g) and  
28  
29 ethylene glycol (1.16 g) have been added and the resulting solution is left to stir for  
30  
31 one night. The amount of acetic acid used, at this step, was calculated as the total  
32  
33 mole number of the acetic acid present in solution equal to 25 times the titanium mole  
34  
35 number.  
36  
37  
38  
39  
40  
41  
42  
43  
44  
45  
46

47 Bi-distilled water (9 ml) has been added to the solution before the deposition on the  
48  
49 different substrates. The details of the synthesis can be found elsewhere [3]. To  
50  
51 obtain thin films, a spin coater, supplied by CaLCTec s.r.l. Model SC10, has been  
52  
53 used. Later on, the films were subjected, for one hour, to a single thermal treatment in  
54  
55 an oven, under ambient atmosphere, at 600°C, with a ramp rate of 25°C/min. The  
56  
57 thickness of the films thus obtained was about 1 μm.  
58  
59  
60

1 Images and microanalyses of PZT powders were made using a Quanta FEG 400  
2  
3  
4 electronic microscope (Fei, The Netherlands). Such PZT powder has been obtained  
5  
6  
7 by scratching the exterior surface of PZT film deposited on the copper layer, so that  
8  
9  
10 to avoid the influence of copper substrate on the measurement. In Fig.1 we report: (a)  
11  
12 a picture of the powder spread on the carbon stab of the SEM; (b) a magnification of  
13  
14 the area on which the microanalyses has been effected and (c) the related  
15  
16  
17 microanalyses. The presence of copper inside the PZT is clearly confirmed by the  
18  
19  
20 line detected at 8keV and 1keV, while Zr, Pb and Ti are visible at 2keV, 2.4keV and  
21  
22  
23 10.5keV and 4.5keV, respectively. The migration of copper ions inside the PZT film  
24  
25  
26 plays an important role on the electric transport properties of the film, to be presented  
27  
28  
29 later. From Fig.1b one can also estimate the roughness of the film  $\sim 0.5\mu\text{m}$ .

30  
31 To measure and investigate the current flow through the PZT film we have used the  
32  
33  
34 setup shown in Fig.2. The copper substrate (henceforth called the copper bottom  
35  
36  
37 electrode) is connected to the output of a voltage source (Wavetek Universal  
38  
39  
40 Waveform Generator model 195). The signal applied to the electrode was a triangular  
41  
42  
43 wave with a wide range of frequencies running from 2.5mHz to 500Hz in four steps  
44  
45  
46 per decade, but with the same voltage amplitude (10V peak to peak). The upper  
47  
48  
49 electrode was a copper cube (1cm edge) placed with one of its optically polished  
50  
51  
52 bases directly in contact to the PZT film (the contact pressure was provided by the  
53  
54  
55 very weight of the copper cube). We have made this choice on purpose lest introduce  
56  
57  
58 a contact voltage between two different materials electrodes. This electrode is  
59  
60  
connected to the ground by a rather small and well known resistor (100 $\Omega$ ). The  
voltages drop on this resistor, measured and recorded by a high input impedance

1 oscilloscope (Agilent Infiniium 54832D MSO), is directly proportional to the electric  
2 current through the PZT film. To minimize the noise, the measuring setup (substrate,  
3 PZT film, upper electrode, and the measuring resistor) was surrounded by a grounded  
4 Faraday cage (not shown in the figure). Another channel of the oscilloscope was used  
5 to visualize and record the applied triangular wave, this last one also serving to  
6 trigger the oscilloscope. For each frequency two sets of data have been recorded,  
7 allowing representing currents and voltages versus time, or currents versus applied  
8 voltage. The digitized sets of data are amenable to several kind of mathematical  
9 processing (for instance: peak area integration, smoothing, curve fitting, etc.). All the  
10 measurements have been performed at room temperature.

### 3. Results

11 The measurements done at 2.5 mHz and 500 Hz are showed in Fig.3 where the  
12 triangular applied voltage (thin line) and the current flowing trough the sample (full  
13 dots) are visible. Two remarkable features can be noticed: i) the strong frequency  
14 dependence of the current flowing through the PZT film; in fact the current measured  
15 at 2.5 mHz (Fig.3a) is sensibly greater than the current measured at 500Hz (Fig.3b);  
16 ii) the semiconductor behaviour of this system, in fact the current flowing through the  
17 PZT film is almost cut for the negative polarity of the applied voltage. Also in Fig.3b  
18 one can see the displacement shift in measured current due to the fact that the applied  
19 voltage varies linearly in time giving birth to a constant current proportional to the  
20 capacitance of the sample and to the rate of the triangular signal. For a 2.5mHz  
21 applied voltage this displacement shift is practically equal to zero, hardly to be seen



in Fig.3a. Subtracting or adding half of this shift, one can get rid of the displacement current and remain only with the conduction current. By plotting this conduction current versus the applied voltage (Fig.4) we obtain a diode like curve in which a hysteresis on the positive side of the graphic is clearly seen.

A first conclusion can be drawn at this stage, namely, the electric conduction through PZT is mainly ionic. At least two facts justify the previous assertion: if the current were electronic there should not have been any difference in the measured currents for 2.5mHz, or 10mHz, 25mHz, etc., the electronic mobilities being quite large in normal electronic conductors. Another fact might be drawn by inspecting the aforementioned displacement shift: let

$$|\Delta i_{displ}| = 2 \frac{dQ}{dt} = 2C \frac{dV}{dt}$$

Knowing  $\frac{dV}{dt}$  (for instance  $\frac{dV}{dt} = 10^4 \frac{V}{s}$  for 500Hz and 10V<sub>pp</sub>) and measuring

$|\Delta i_{displ}|$  (170μA from Fig.3b) the capacitance  $C$  is estimated to be  $C = 1.7 \times 10^{-8} F$  and the relative permittivity is about 7, typical for a solid dielectric (ferroelectric).

To obtain more information about the accumulating charge process that is responsible to the hysteresis, the positive increasing side (one quarter of the period) has been analyzed separately for each frequency and all of these plots have been fitted with the equation

$$I(T, V) = a + bV^m \quad (1)$$

connecting the current intensity  $I$  to the period  $T$  by means of the parameter  $b$  ( $a$  gives just a shift of zero and it is not interesting), and to the applied voltage  $V$ , while  $m$  is a constant. For all the plots a very good agreement with the experimental curve has been obtained. In Fig. 5 (a and b) the  $I$ - $V$  plots (black dots) for the lowest frequency value of the applied voltage (2.5 mHz) and for a higher one (250 Hz) both fitted with the equation 1 (white continuous line) are reported, respectively. To get the relation between  $b$  and  $T$  the fitted values of the parameter  $b$  have been plotted with respect to  $T$  (see Fig.6) and a good simple fitting function has been found

$$b(T) = \alpha + \beta T^\gamma \quad (2)$$

where  $\alpha=4.75 \cdot 10^{-8}$ ,  $\beta=2.60 \cdot 10^{-8}$ ,  $\gamma=0.25$ . Using the equation (1) it is possible to find the displaced charge  $Q$

$$Q = \int_0^{T/4} I dt = \frac{1}{v} \int_0^{V_0} (a + bV^m) dV = \frac{T}{4V_0} \left( aV_0 + \frac{b}{m} V_0^{m+1} \right) = \left( \frac{a}{4} + \frac{bV_0^m}{4m} \right) T \quad (3)$$

where we used the fact that for the triangular voltage one has  $V(t) = v t$ ,  $dt = \frac{1}{v} dV$ . As

for  $t = T/4 \Rightarrow V = V_0$ , we have  $\frac{1}{v} = \frac{T}{4V_0}$ ,  $V_0$  being the amplitude of the triangular signal.

Now, using the equation (2) one gets

$$Q = \frac{T}{4} \left( a + (\alpha + \beta T^\gamma) \frac{V_0^m}{m} \right) = pT + qT^{\gamma+1} \quad (4)$$

where  $p \equiv \frac{a}{4} + \frac{\alpha V_0^m}{m}$  and  $q \equiv \frac{\beta V_0^m}{m}$ .

Of course, the values  $p$  and  $q$  computed with  $a$ ,  $\alpha$ ,  $\beta$ ,  $m$ ,  $V_0$  should be consistent only with the charge displaced during a quarter of a period, not with the accumulated hysteresis charge, but the order of magnitude should be the same. Finally we have been conducted to use the fitting function

$$Q = pT + qT^{1.25} \quad (5)$$

to fit the plot of the accumulated charge in function of the period (that is the included area of the hysteresis calculated for different values of the applied voltage frequency yielding an excellent agreement (see Fig.7).

#### 4. Discussion and conclusions

The constant  $m$  in Eq(1) turned out to be  $m \approx \frac{7}{3}$ . As a matter of fact  $V^m$  dependence of  $I$  is not unusual in physics. (The simplest example being Ohm's law where  $m$  is, of course, 1). In our case  $V^{\frac{7}{3}}$  law should be a consequence of the transport mechanism across the PZT film. The parameter  $b$  is linked to the carrier density and it should depend on the liberation of new carriers, in time. As already argued, these carriers should have low mobility, i.e. they are ions, presumably  $Cu^+$  or  $Cu^{2+}$ , as the

1 microanalyses clearly show (Fig.1c). The liberation and the re-absorption of carriers  
2  
3  
4 are slow processes, connected also to the internal electric field.  
5

6 For each value of the voltage across the sample should be a characteristic time for  
7  
8 free carriers to reach the new equilibrium value. If the sweeping time (that is  $T/4$ ) of  
9  
10 the voltage is smaller than the characteristic time, the carrier concentration does not  
11  
12 reach saturation. Contrary, decreasing the voltage (the next  $1/4$  of a period) the  
13  
14 accumulated charge carriers do not have enough time to diminish toward the  
15  
16 equilibrium value, so the decreasing of the current does not follow the same path as  
17  
18 the increasing current and this asymmetry creates the hysteresis charge. A rather large  
19  
20 value of  $m$  indicated a thermal activated 3D hopping process [7].  
21  
22  
23  
24  
25  
26  
27

28 The rectifying effect is closely connected to the large number of copper ions  
29  
30 dissolved in the PZT side of the interface during the thermal treatment (see Fig.1c,  
31  
32 again).  
33  
34  
35

36 A sketch of the process is presented in Fig.8 and Fig.9. The absorbed copper ions  
37  
38 form a positive layer within PZT right at the interface, while a negative charge  
39  
40 (electrons) appears in the copper base interface to make the sample electrically  
41  
42 neutral. A positive voltage on the copper base withdraws electrons from the  
43  
44 compensating layer leaving the positive copper ions to diffuse into the bulk. So the  
45  
46 concentration of positive charge on the opposite side of PZT increases thus attracting  
47  
48 electrons from the ground across the measuring resistor. A negative voltage on the  
49  
50 copper base narrows the positive ionic distribution in PZT stabilizing it and no  
51  
52 positive charge is injected to the opposite side of PZT to produce a measurable  
53  
54  
55  
56  
57  
58  
59  
60

1 current across the resistor. To be sure the positive copper ions diffusion into the bulk  
2  
3  
4 is a very slow process, thus accounting for the frequency dependence of the current.  
5  
6  
7 Also, for practical purposes this small, but not at all negligible solubility of the  
8  
9  
10 substrate into the PZT layer should be taken into account.  
11  
12  
13  
14  
15  
16  
17  
18  
19  
20  
21  
22  
23  
24  
25  
26  
27  
28  
29  
30  
31  
32  
33  
34  
35  
36  
37  
38  
39  
40  
41  
42  
43  
44  
45  
46  
47  
48  
49  
50  
51  
52  
53  
54  
55  
56  
57  
58  
59  
60

For Peer Review Only

## References

- [1] C.T. Lin, B.W. Scanlan, J.D. McNeill, J.S. Webb, Li Li, R.A. Lipeles, P.M. Adams, M.S. Leung: Crystallization behavior in a low temperature acetate process for perovskite  $\text{PbTiO}_3$ ,  $\text{Pb}(\text{Zr}, \text{Ti})\text{O}_3$ , and  $(\text{Pb}_{1-x}, \text{La}_x)(\text{Zr}_y, \text{Ti}_{1-y})_{1-x/4}\text{O}_3$  bulk powders. *J. Mater. Res.* 7(9), 2546 (1992).
- [2] S. S. Dana, K. F. Etzold, and J. Clabes: Crystallization of sol-gel derived lead zirconate titanate thin films. *J. Appl. Phys* 69(8), 4398 (1991).
- [3] S. Marino, M. Castriota, G. Strangi, E. Cazzanelli, N. Scaramuzza: Asymmetric nematic liquid crystal cells containing lead zirconium titanate PZT films: *Journal of Applied Physics*. **102** 013112 (2007). Selected for *Virtual Journal of Nanoscale Science & Technology* July 30, 2007.
- [4] Gouji Asano, Hitoshi Morioka, Hiroshi Funakubo, Tetsuo Shibutami, and Noriaki Oshima: Fatigue-free  $\text{RuO}_2/\text{Pb}(\text{Zr}, \text{Ti})\text{O}_3/\text{RuO}_2$  capacitor prepared by metalorganic chemical vapor deposition at 395 °C. *Appl. Phys. Lett.* **83**, 1512 (2003).
- [5] B. S. Kang, D. J. Kim, J. Y. Jo, T. W. Noh, Jong-Gul Yoon, T. K. Song, Y. K. Lee, J. K. Lee, S. Shin, and Y. S. Park: Polarization retention in  $\text{Pb}(\text{Zr}_{0.4}\text{Ti}_{0.6})\text{O}_3$  capacitors with  $\text{IrO}_2$  top electrodes. *Appl. Phys. Lett* 84, 3127 (2004).
- [6] E. Bruno, M.P. De Santo, M. Castriota, S. Marino, G. Strangi, E. Cazzanelli, and N. Scaramuzza: Morphological and electrical investigations of lead zirconium titanate thin films obtained by sol-gel synthesis on indium tin oxide electrodes. *Journal of Applied Physics*. **103**, 064103 (2008).
- [7] N.F. Mott, E.A. Davis, *Electronic Processes in Non Crystalline Materials*, 2<sup>nd</sup> edn. (Oxford: Clarendon, 1979).

## Figure captions

Figure 1: Picture of PZT powder spread on the SEM carbon stab (a), magnification of the small square area shown in (a) and the related microanalyses (c).

Figure 2: Experimental setup;  $r$  – the measuring resistor (100  $\Omega$ ).

Figure 3: The current through the PZT/copper sample when a triangular wave is applied. The frequency of the applied voltage: (a) 2.5mHz; (b): 500Hz.

Figure 4: A typical current – voltage plot showing the hysteresis for positive voltages and rectification for negative voltages.

Figure 5: Current – voltage plots of the increasing ramp of the applied voltage at 2.5mHz (a) and 250Hz (b). The black dots are the experimental points and the white line is the fitting curve.

Figure 6: The plot of parameter  $b$  versus period  $T$ . The open squares are the experimental points and the black line is the fitting curve.

Figure 7: Charge in function of period. The open squares are the experimental points and the black line is the fitting curve.

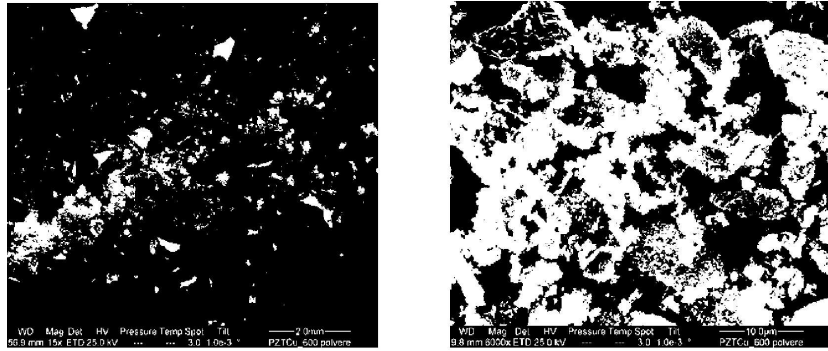
1 Figure 8: (a) Equilibrium distribution of copper ions in PZT and the counter electrons  
2  
3 in the copper base electrode; (b) copper base electrode under positive voltage; (c)  
4  
5 copper base electrode under negative voltage.  
6  
7  
8  
9

10  
11 Figure 9: Densities of charge carriers at copper base, PZT, and collecting copper  
12  
13 electrode: (a) no voltage; (b) positive voltage; (c) negative voltage, as before.  
14  
15  
16  
17  
18  
19  
20  
21  
22  
23  
24  
25  
26  
27  
28  
29  
30  
31  
32  
33  
34  
35  
36  
37  
38  
39  
40  
41  
42  
43  
44  
45  
46  
47  
48  
49  
50  
51  
52  
53  
54  
55  
56  
57  
58  
59  
60

For Peer Review Only

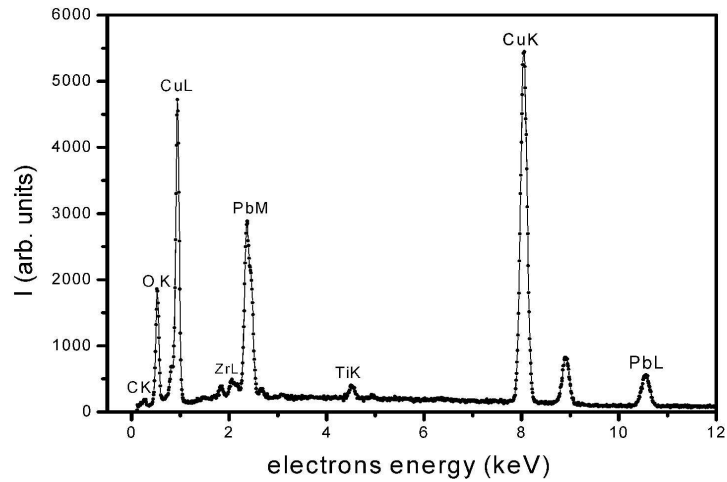


1  
2  
3  
4  
5  
6  
7  
8  
9  
10  
11  
12  
13  
14  
15  
16  
17  
18  
19  
20  
21  
22  
23  
24  
25  
26  
27  
28  
29  
30  
31  
32  
33  
34  
35  
36  
37  
38  
39  
40  
41  
42  
43  
44  
45  
46  
47  
48  
49  
50  
51  
52  
53  
54  
55  
56  
57  
58  
59  
60



a)

b)



c)

FIGURE 1

168x246mm (500 x 500 DPI)

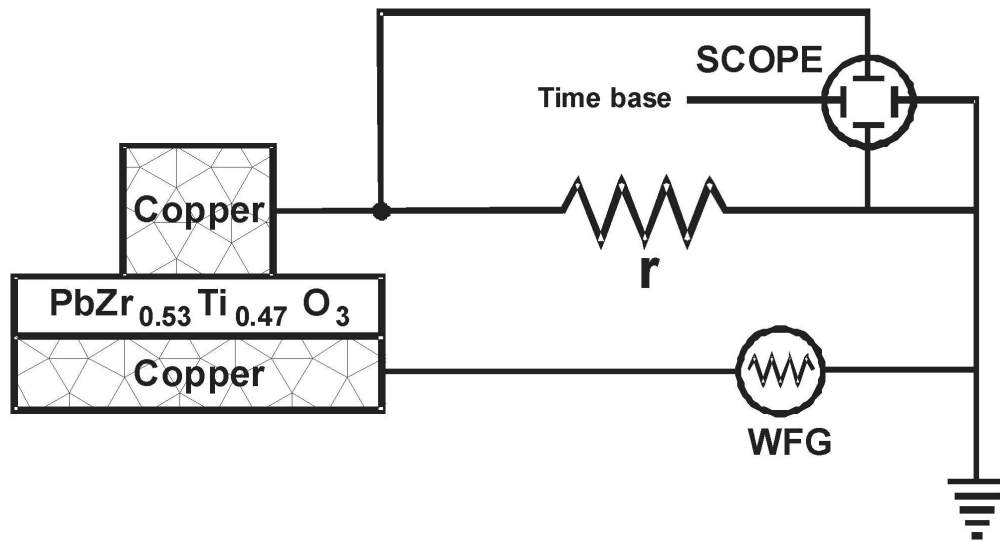


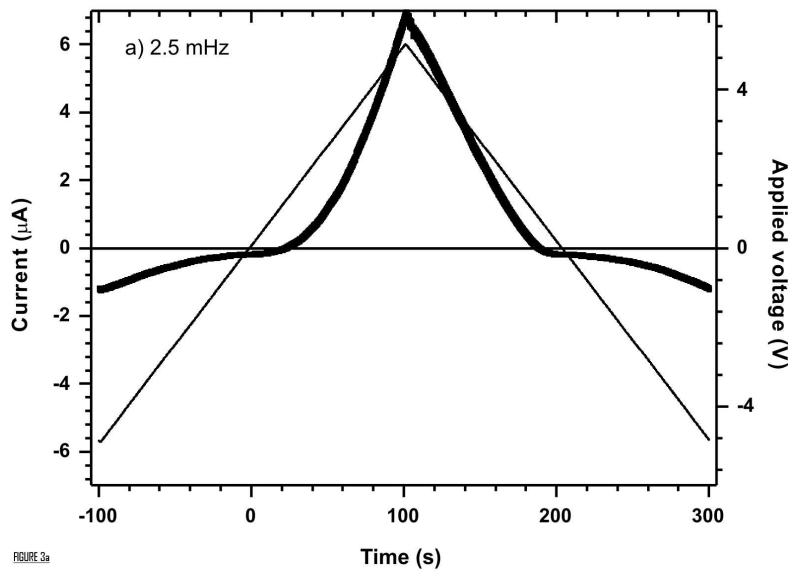
FIGURE 2

169x115mm (300 x 300 DPI)

view Only

1  
2  
3  
4  
5  
6  
7  
8  
9  
10  
11  
12  
13  
14  
15  
16  
17  
18  
19  
20  
21  
22  
23  
24  
25  
26  
27  
28  
29  
30  
31  
32  
33  
34  
35  
36  
37  
38  
39  
40  
41  
42  
43  
44  
45  
46  
47  
48  
49  
50  
51  
52  
53  
54  
55  
56  
57  
58  
59  
60

1  
2  
3  
4  
5  
6  
7  
8  
9  
10  
11  
12  
13  
14  
15  
16  
17  
18  
19  
20  
21  
22  
23  
24  
25  
26  
27  
28  
29  
30  
31  
32  
33  
34  
35  
36  
37  
38  
39  
40  
41  
42  
43  
44  
45  
46  
47  
48  
49  
50  
51  
52  
53  
54  
55  
56  
57  
58  
59  
60



414x638mm (96 x 96 DPI)

1  
2  
3  
4  
5  
6  
7  
8  
9  
10  
11  
12  
13  
14  
15  
16  
17  
18  
19  
20  
21  
22  
23  
24  
25  
26  
27  
28  
29  
30  
31  
32  
33  
34  
35  
36  
37  
38  
39  
40  
41  
42  
43  
44  
45  
46  
47  
48  
49  
50  
51  
52  
53  
54  
55  
56  
57  
58  
59  
60

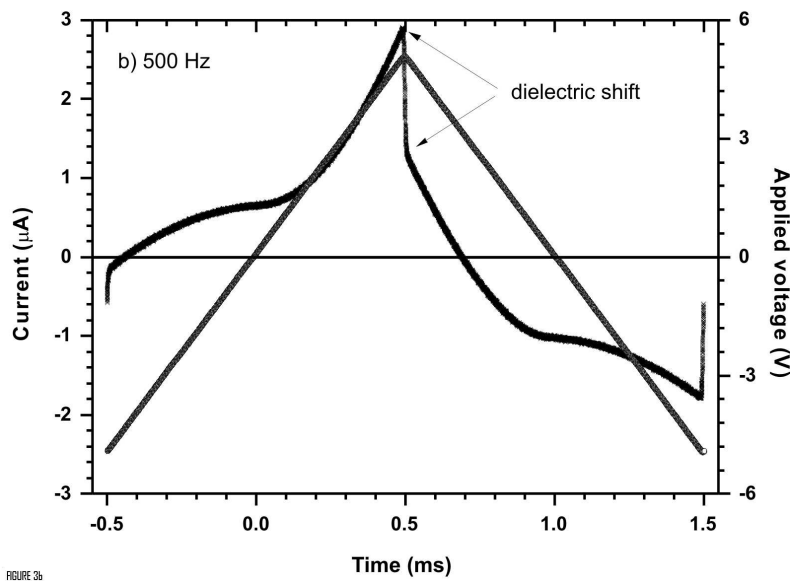


FIGURE 3b

420x639mm (96 x 96 DPI)

1  
2  
3  
4  
5  
6  
7  
8  
9  
10  
11  
12  
13  
14  
15  
16  
17  
18  
19  
20  
21  
22  
23  
24  
25  
26  
27  
28  
29  
30  
31  
32  
33  
34  
35  
36  
37  
38  
39  
40  
41  
42  
43  
44  
45  
46  
47  
48  
49  
50  
51  
52  
53  
54  
55  
56  
57  
58  
59  
60

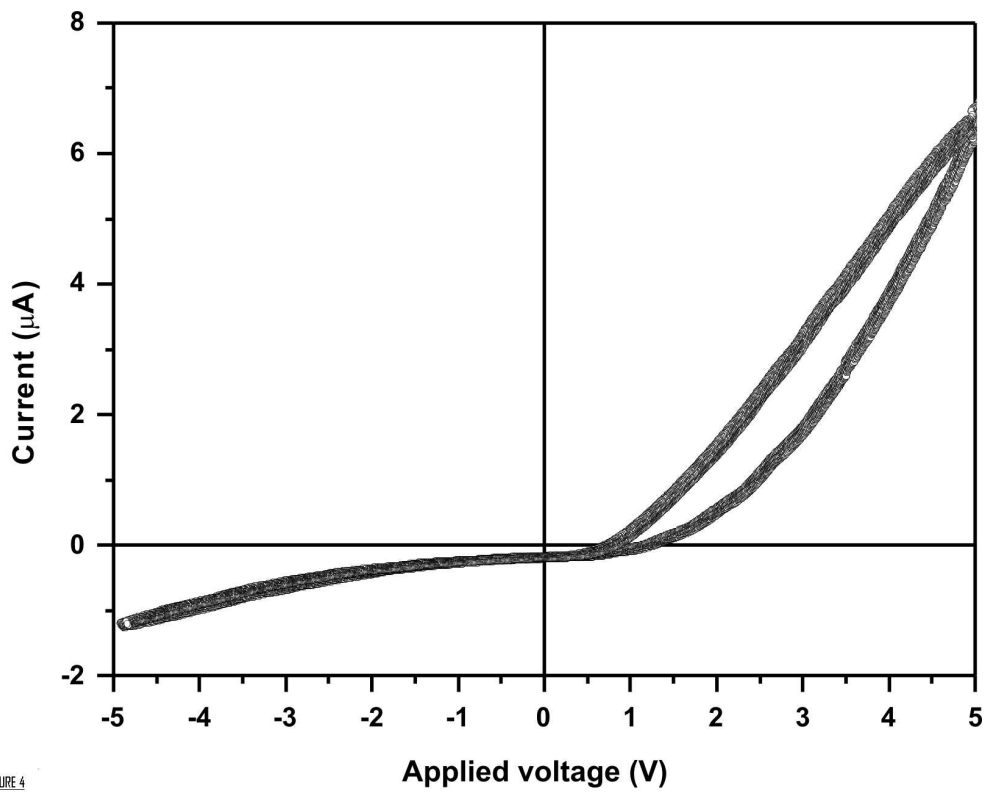


FIGURE 4

433x340mm (96 x 96 DPI)

ew Only

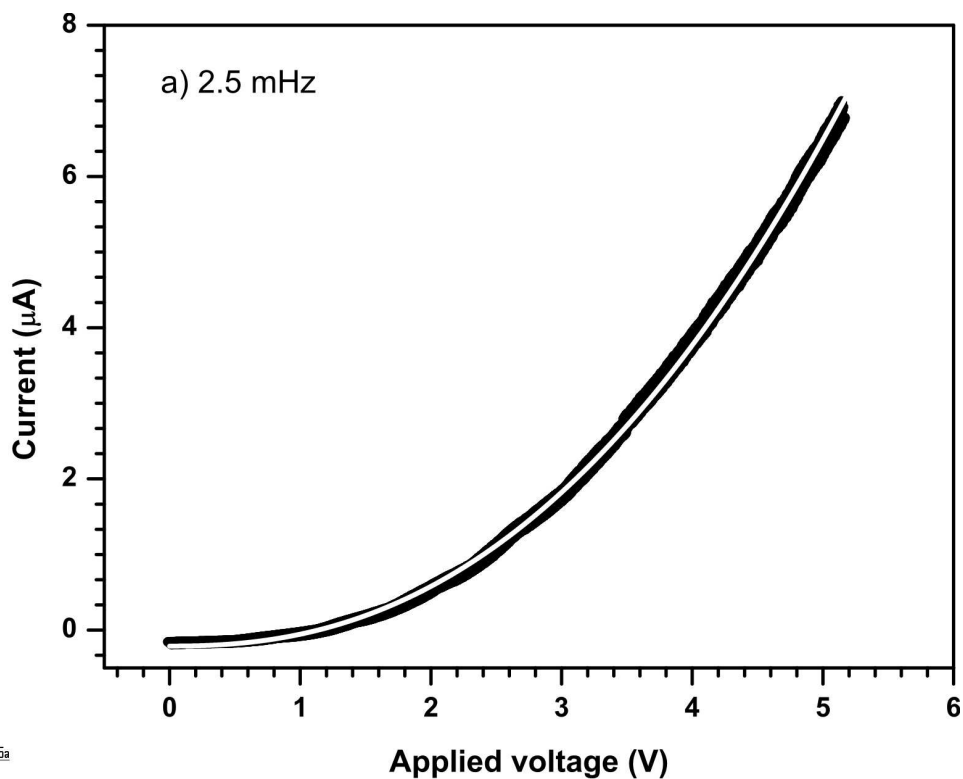


FIGURE 5a

429x333mm (96 x 96 DPI)

ew Only

1  
2  
3  
4  
5  
6  
7  
8  
9  
10  
11  
12  
13  
14  
15  
16  
17  
18  
19  
20  
21  
22  
23  
24  
25  
26  
27  
28  
29  
30  
31  
32  
33  
34  
35  
36  
37  
38  
39  
40  
41  
42  
43  
44  
45  
46  
47  
48  
49  
50  
51  
52  
53  
54  
55  
56  
57  
58  
59  
60

1  
2  
3  
4  
5  
6  
7  
8  
9  
10  
11  
12  
13  
14  
15  
16  
17  
18  
19  
20  
21  
22  
23  
24  
25  
26  
27  
28  
29  
30  
31  
32  
33  
34  
35  
36  
37  
38  
39  
40  
41  
42  
43  
44  
45  
46  
47  
48  
49  
50  
51  
52  
53  
54  
55  
56  
57  
58  
59  
60

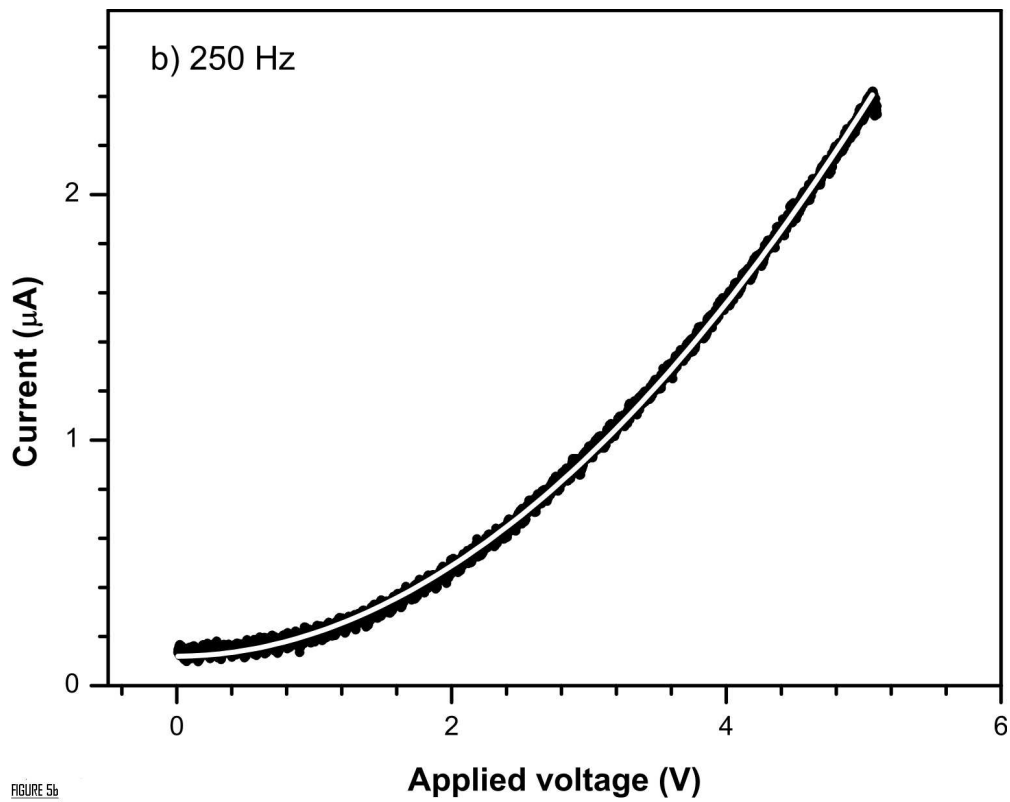
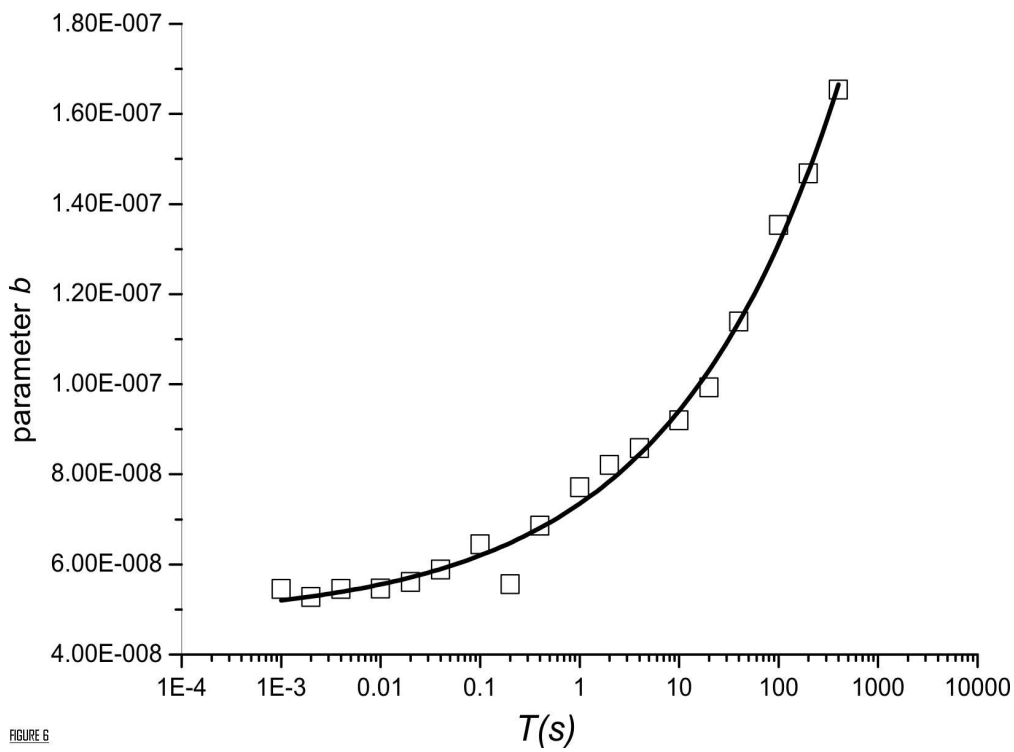


FIGURE 5b

408x326mm (96 x 96 DPI)

View Only



431x316mm (96 x 96 DPI)

new Only

1  
2  
3  
4  
5  
6  
7  
8  
9  
10  
11  
12  
13  
14  
15  
16  
17  
18  
19  
20  
21  
22  
23  
24  
25  
26  
27  
28  
29  
30  
31  
32  
33  
34  
35  
36  
37  
38  
39  
40  
41  
42  
43  
44  
45  
46  
47  
48  
49  
50  
51  
52  
53  
54  
55  
56  
57  
58  
59  
60



1  
2  
3  
4  
5  
6  
7  
8  
9  
10  
11  
12  
13  
14  
15  
16  
17  
18  
19  
20  
21  
22  
23  
24  
25  
26  
27  
28  
29  
30  
31  
32  
33  
34  
35  
36  
37  
38  
39  
40  
41  
42  
43  
44  
45  
46  
47  
48  
49  
50  
51  
52  
53  
54  
55  
56  
57  
58  
59  
60

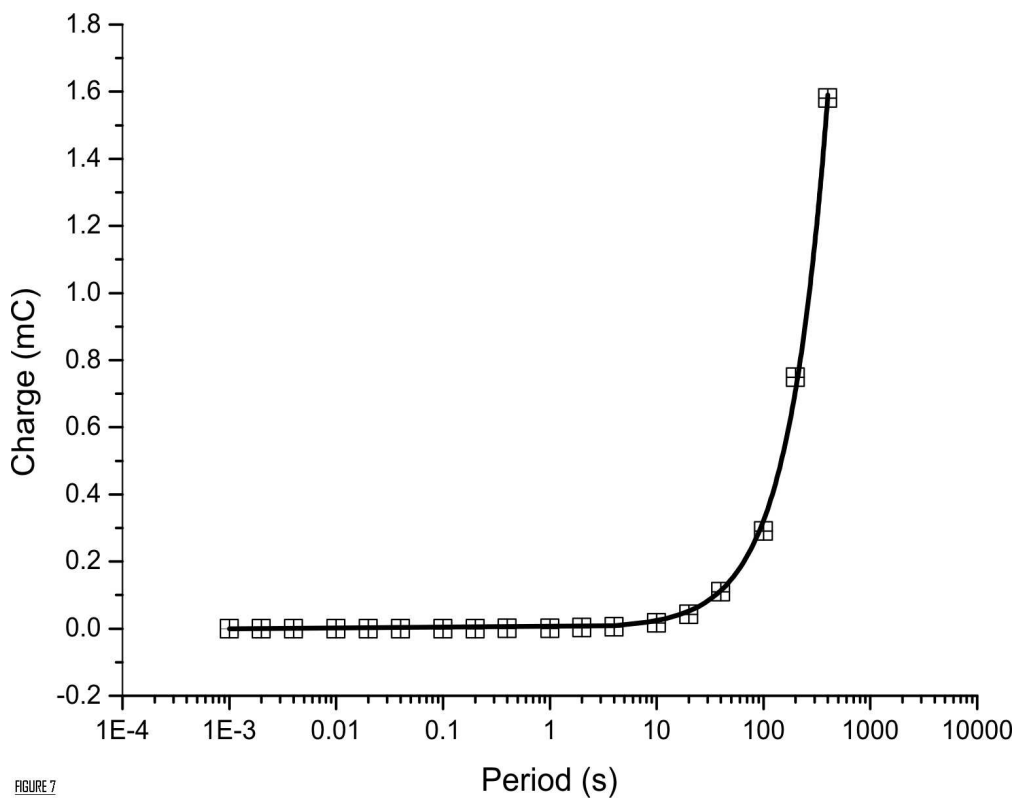


FIGURE 7

404x317mm (96 x 96 DPI)

Pre-proof Only

1  
2  
3  
4  
5  
6  
7  
8  
9  
10  
11  
12  
13  
14  
15  
16  
17  
18  
19  
20  
21  
22  
23  
24  
25  
26  
27  
28  
29  
30  
31  
32  
33  
34  
35  
36  
37  
38  
39  
40  
41  
42  
43  
44  
45  
46  
47  
48  
49  
50  
51  
52  
53  
54  
55  
56  
57  
58  
59  
60

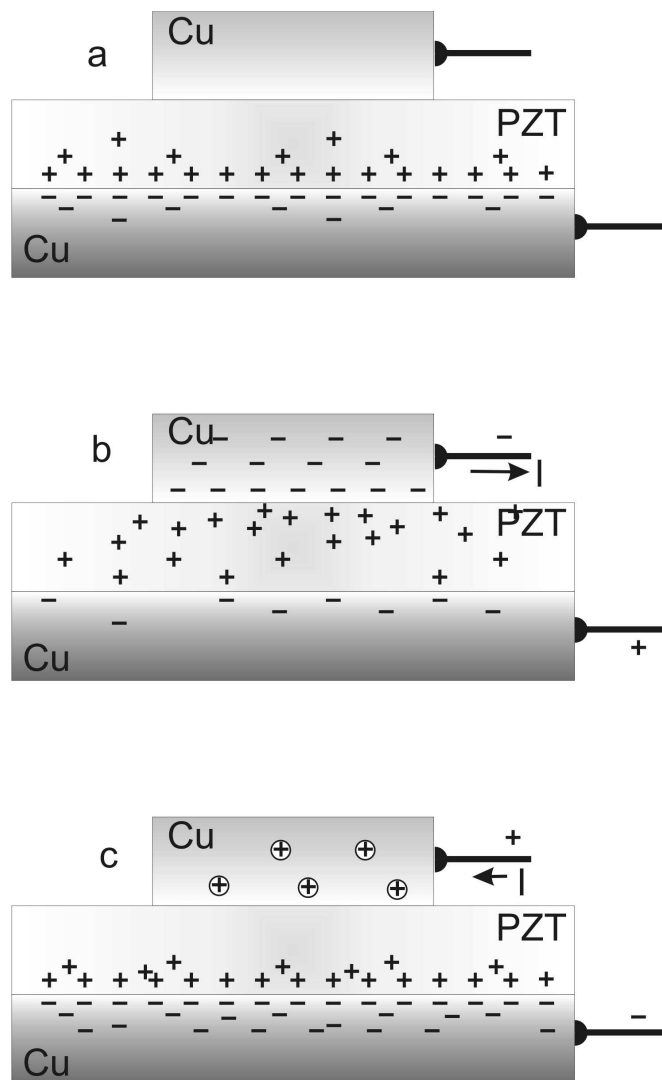
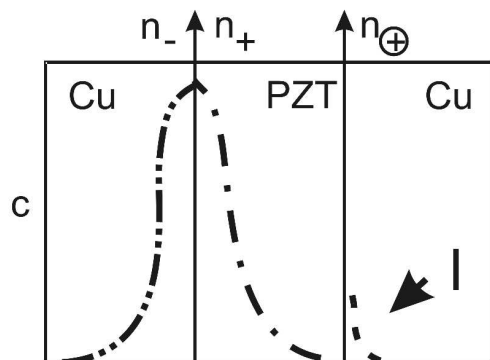
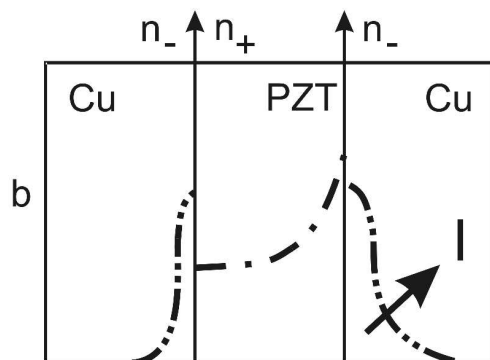
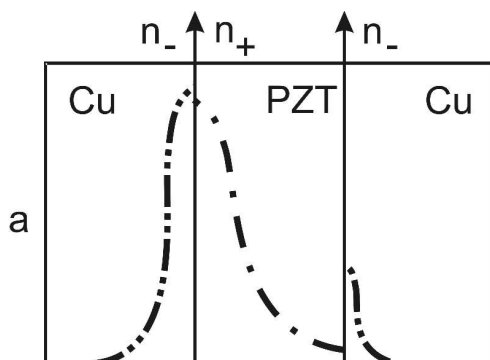


FIGURE 9

422x717mm (96 x 96 DPI)

1  
2  
3  
4  
5  
6  
7  
8  
9  
10  
11  
12  
13  
14  
15  
16  
17  
18  
19  
20  
21  
22  
23  
24  
25  
26  
27  
28  
29  
30  
31  
32  
33  
34  
35  
36  
37  
38  
39  
40  
41  
42  
43  
44  
45  
46  
47  
48  
49  
50  
51  
52  
53  
54  
55  
56  
57  
58  
59  
60



538x1034mm (96 x 96 DPI)